AD-A259 886

DTIC
ELECTE
FEB 5 1993

Solar-Powered Light Emitting Diode Power Line Avoidance Marker Design

By

Ellen H. Snook
Clarence E. Rash
John S. Martin
Richard R. Levine

Sensory Research Division

Parley P. Johnson
James A. Lewis
John H. Hapgood

Research Systems Division

93-02008

December 1992

93 23 015

Notice

<u>Qualified requesters</u>

Qualified requesters may obtain copies from the Defense Technical Information Center (DTIC), Cameron Station, Alexandria, Virginia 22314. Orders will be expedited if placed through the librarian or other person designated to request documents from DTIC.

<u>Change of address</u>

Organizations receiving reports from the U.S. Army Aeromedical Research Laboratory on automatic mailing lists should confirm correct address when corresponding about laboratory reports.

<u>Disposition</u>

Destroy this report when it is no longer needed. Do not return to the originator.
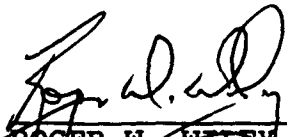
<u>Disclaimer</u>

The views, opinions, and/or findings contained in this report are those of the author(s) and should not be construed as an official Department of the Army position, policy, or decision, unless so designated by other official documentation. Citation of trade names in this report does not constitute an official Department of the Army endorsement or approval of the use of such commercial items.

Reviewed:

RICHARD R. LEVINE
LTC, MS
Director, Sensory Research
  Division

Released for publication:

ROGER W. WILEY, O.D., Ph.D.
Chairman, Scientific
  Review Committee

DAVID H. KARNEY
Colonel, MC, SFS
Commanding

REPORT DOCUMENTATION PAGE					Form Approved OMB No 0704-0188

1a. REPORT SECURITY CLASSIFICATION Unclassified		1b RESTRICTIVE MARKINGS			

2a. SECURITY CLASSIFICATION AUTHORITY	3 DISTRIBUTION / AVAILABILITY OF REPORT
2b. DECLASSIFICATION / DOWNGRADING SCHEDULE	Approved for public release; distribution unlimited

4. PERFORMING ORGANIZATION REPORT NUMBER(S) USAARL Report No. 93-6	5. MONITORING ORGANIZATION REPORT NUMBER(S)

6a. NAME OF PERFORMING ORGANIZATION U.S. Army Aeromedical Research Laboratory	6b. OFFICE SYMBOL (If applicable) SGRD-UAS-VS	7a. NAME OF MONITORING ORGANIZATION U.S. Army Medical Research and Development Command

6c. ADDRESS (City, State, and ZIP Code) P.O. Box 577 Fort Rucker, AL 36362-5292	7b. ADDRESS (City, State, and ZIP Code) Fort Detrick Frederick, MD 21702-5012

8a. NAME OF FUNDING / SPONSORING ORGANIZATION	8b. OFFICE SYMBOL (If applicable)	9. PROCUREMENT INSTRUMENT IDENTIFICATION NUMBER

8c. ADDRESS (City, State, and ZIP Code)	10 SOURCE OF FUNDING NUMBERS			
	PROGRAM ELEMENT NO. 0602787A	PROJECT NO. 3M162 787879	TASK NO. BC	WORK UNIT ACCESSION NO 164

11. TITLE (Include Security Classification)

(U) Solar-Powered Light Emitting Diode Power Line Avoidance Marker Design

12. PERSONAL AUTHOR(S) Snook, Ellen H.; Rash, Clarence E.; Martin, John S.; Levine, Richard R.;
Johnson, Parley P.; Lewis, James A.; Hapgood, John H.

13a. TYPE OF REPORT Final	13b. TIME COVERED FROM _____ TO _____	14. DATE OF REPORT (Year, Month, Day) 1992 December	15. PAGE COUNT 25

16. SUPPLEMENTARY NOTATION

17.		COSATI CODES	18. SUBJECT TERMS (Continue on reverse if necessary and identify by block number)
FIELD	GROUP	SUB-GROUP	wire marker, light emitting diode, solar power, aided and unaided flights
20	06		
23	02		

19. ABSTRACT (Continue on reverse if necessary and identify by block number)

In-flight wire strikes are a constant threat to U.S. Army Aviation during all-weather, daytime and nighttime helicopter operations. Despite routine training on wire avoidance techniques, wire strikes continue to occur, with a majority of the mishaps historically occurring during training and maneuvering over familiar sites. In an effort to increase the conspicuity of suspended cables and wires, the aviation training community at Fort Rucker, Alabama, currently employs a passive wire marking system which consists of international-orange colored spheres suspended from cables and wires in heavily trafficked airspace. During a previous evaluation of wire marker visibility, a solar-powered wire marker design was developed. This new design incorporates retroreflective material and light emitting diodes (LEDs) to provide greater range visibility and detectability during aided and unaided flight.

20. DISTRIBUTION / AVAILABILITY OF ABSTRACT ☒ UNCLASSIFIED/UNLIMITED ☐ SAME AS RPT. ☐ DTIC USERS	21 ABSTRACT SECURITY CLASSIFICATION Unclassified
22a. NAME OF RESPONSIBLE INDIVIDUAL Chief, Scientific Information Center	22b TELEPHONE (Include Area Code) 205-255-6907	22c. OFFICE SYMBOL SGRD-UAX-SI

DD Form 1473, JUN 86　　Previous editions are obsolete.

Table of contents

DTIC QUALITY INSPECTED 3

List of figures

List of tables

Acknowledgments

==

This page intentionally left blank.

==

Introduction

In-flight wire strikes are a serious threat to U.S. Army aviation in all weather conditions during daytime and nighttime operations such as terrain flight, enclosed area takeoff and landing, and confined area manuevering. Historically, the majority of wire strikes have occurred over familiar sites and during training missions. Despite aviator training on wire avoidance techniques, U.S. Army peacetime wire strikes, with the resultant loss of aircraft, loss of life, or injuries, remain a serious problem.

The aviation training community at Fort Rucker, Alabama, currently employs a passive marking system for increasing the conspicuity of high tension cables, electrical power lines, and telephone wires. This system uses international-orange fiberglass spheres having a diameter of approximately 11.5 inches. These spheres are attached to the cables and wires in areas heavily used by aircraft (Figure 1).

In May 1990, the U.S. Army Aeromedical Research Laboratory evaluated the current wire marker design (Figure 2a), a modification of the current design, and alternate designs for day/night conspicuity. Figure 2b shows the modified basic design which was the current sphere with 1.5 inch wide, white, high-reflectivity tape applied in a cross pattern. The alternative designs, shown in Figures 2c and 2d, had a polyhedronal shaped shell, international orange in color. One alternative marker had no additional markings (Figure 2c); one was marked with 2.5 inch diameter, circular pieces of white 3M Scotchlite[TM] retro-reflective tape applied to the individual faces of the polyhedron (Figure 2d); and the other was marked similarly, but with yellow-colored retroreflective tape.

Day conspicuity was performed with the naked eye, while night conspicuity included the use of image intensification (I^2) devices as well as the naked eye. Results of this previous study (Levine, Rash, and Martin, 1991) demonstrated both viewing- and lighting-specific effects for each of the marker designs tested. While no differences in detection range among designs were observed under daylight conditions, improved performance under several viewing/lighting conditions was observed for the retroreflective polyhedron designs under typical aircraft lighting conditions at night. Increased detection ranges were noted both with and without I^2 devices and under aircraft lighting conditions characteristic of the local aviation training environment.

----

*See Appendix A.

1

Figure 1.   Current basic wire marker (international-orange
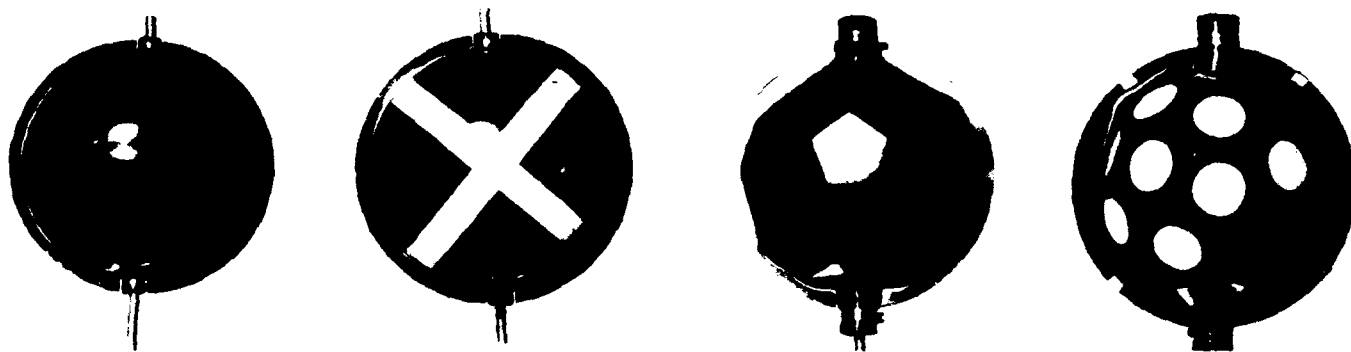sphere) mounted on power line.

Figure 2.   Wire marker test designs: (a) current uniform sphere,
(b) modified sphere with reflective tape in a cross
(X) pattern, (c) uniform polyhedron, (d) polyhedron
with circular retroreflective tape.

Table 1.

Mean detection distances (in feet)
for conventional wire marker designs
(Levine, Rash, and Martin, 1991)

	Basic design	Modified basic design	Reflective polyhedron design
Day, unaided	4200*	4200*	4200*
Night, unaided			
Position lights	125	488	750
Anticollision lights	213	688	1225
Searchlight	1200	4200*	4200*
Blackout	63	125	138
Night, I^2 2nd			
Position lights	450	1250	1975
Infrared searchlight	525	1375	1975
Blackout	750	825	850
Night, I^2 3rd			
Position lights	475	1425	2050
Infrared searchlight	575	1600	2250
Blackout	750	825	950

* Note: Maximum available range was 4200 feet.

Data in Table 1 summarize the results of the 1991 study.
Mean detection distances are presented for day/night and
unaided/aided viewing conditions. (Note: It should be emphasized
that, because of the benign and relatively static conditions
under which the data were collected, it may be erroneous to use
the ranges in the data table as typical detection distances under
training or operational conditions.)

A range ceiling, which existed due to restricted test space (4200 feet maximum working distance), prevented discrimination between designs for the daytime conditions. Thus, there were no observed differences in daytime detection distances among any of the tested markers within the test space. However, at a range of 4200 feet, the 11.5 inch overall diameter of the various marker designs subtended an angle of about 23.0 arc seconds. The 1.5- and 2.5-inch pieces of retroreflective tape used for visibility enhancement subtended angles of 3.0 and 5.0 arc seconds, respectively. It was suggested that detection at this range was primarily a function of color (international orange) and contrast (lighter object against a darker tree line), rather than specular refection or detail on the surface of the shell. Therefore, differences in detectability among the marker designs would not be observed at distances greater than 4200 feet. However, heightened conspicuity could result from differences in specular reflectivity of a mobile target or when viewing from a mobile platform.

Three viewing systems were used for night testing, i.e., the unaided eye, the AN/PVS-5 night vision goggle (2nd generation I^2), and the Aviator's Night Vision Imaging System-ANVIS (3rd generation I^2). Each of these systems has a different spectral sensitivity. With all of these systems, the detection range of the various designs depends on the level of light, the spectral distribution of the ambient lighting, and the spectral reflective properties of the markers.

For unaided viewing in the presence of artificial lighting in the form of aircraft position and anticollision lights, the modified and alternative designs using reflective material provided the greatest detection ranges with the retroreflective polyhedron design providing nearly twice the range of the modified basic design. Under the increased directional output provided by the searchlight, the range ceiling prevented discrimination among the reflective designs -- all were equally detectable out to the maximum test range of 4200 feet. Under blackout conditions, with moonlight as the principal source of illumination, detectability among designs was considerably reduced and nearly equivalent.

Similar trends in the data were observed with I^2 devices, either 2nd (AN/PVS-5) or 3rd generation (ANVIS) image intensification systems. With the aircraft's position lights on steady dim or illuminated with the infrared searchlight, detection ranges with the retroreflective polyhedrons generally were superior to the basic design. Under normal low-light ambient conditions ("blackout"), no significant advantage in detectability was observed among any of the tested designs.

4

It is erroneous to use the ranges in the data table as absolute detection distances. However, it may be generalized that the detection range values associated with the test designs would be considered inadequate for all unaided flight conditions except for the use of the aircraft searchlight (and then only within its footprint). In addition, these designs provide only minimal increases in detection ranges for aided nighttime flight using image intensifiers.

In summary, the detection range data in Table 1 show improved detectability performance for the retroreflective polyhedron design over the current basic design for all viewing conditions. However, performance for this design was maximum (although range limited) only for unaided daytime and unaided nighttime searchlight conditions. In an attempt to achieve maximum performance for all nighttime conditions, a new wire marker design was sought. The resulting design (patent pending) features light emitting diodes (LEDs) in conjunction with retroreflective markers. This alternative design is intended to provide maximum performance for all daytime and nighttime conditions.

Technical description

System description and operation

The alternative wire marker design is intended to facilitate naked eye and electro-optical image intensification detection in daytime and nighttime/inclement weather through the use of an enhanced visual detection scheme. Enhanced detectability is achieved through the use of surface mounted retroreflective tape marking and LEDs (red or infrared). The wire marker shell is constructed of a weather resistant material, polyhedronal shaped, and international orange in color. The shell serves as the housing for the internal power supply, electronic circuit board, and LED wiring harness. Figures 3 and 4 show exterior and interior views of the wire marker.

The operation of the solar powered LED wire marker is depicted in a functional block diagram in Figure 5. The functional blocks include a power supply (with power collecting, power storage, and power distribution sections), a light level detector, a power supply voltage monitor, a logic control circuit, and a visibility enhancement module.

The wire marker operates in two modes, daytime mode and nighttime/inclement weather mode, with the light level detector serving as the mode selector. When the ambient light level reaches a minimum threshold for daytime operation, the light level detector sends the appropriate signal to the logic control circuit to shut down the LED flasher circuit in the visual
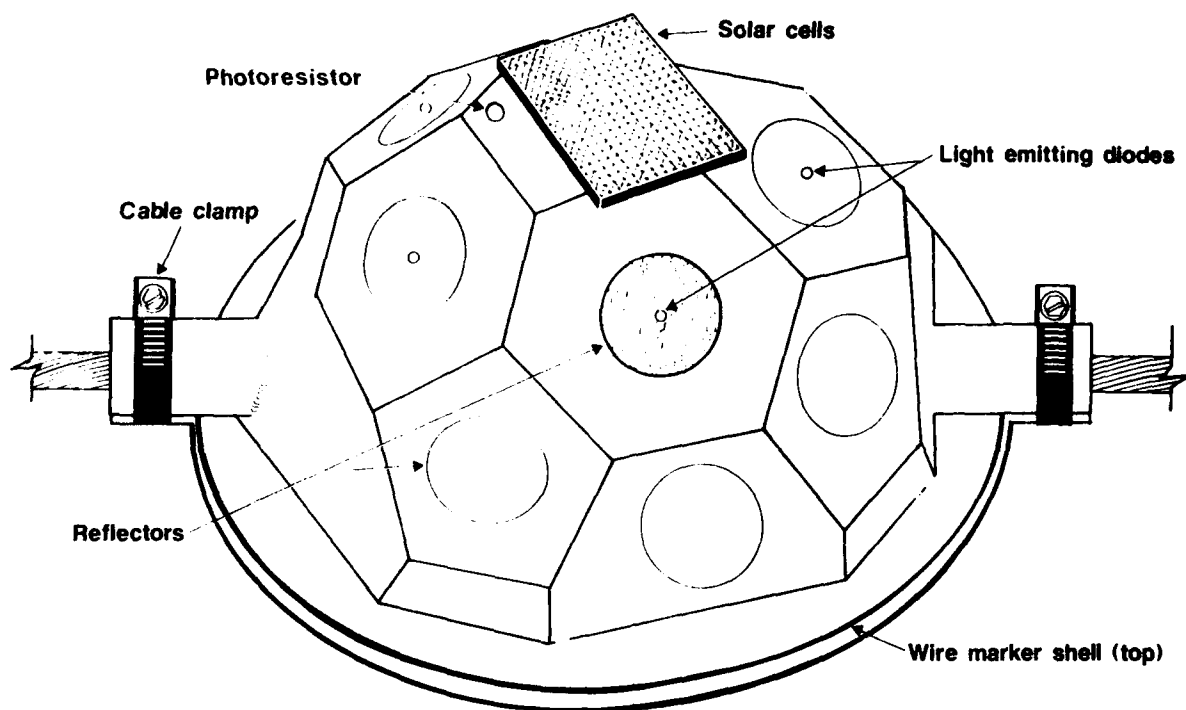
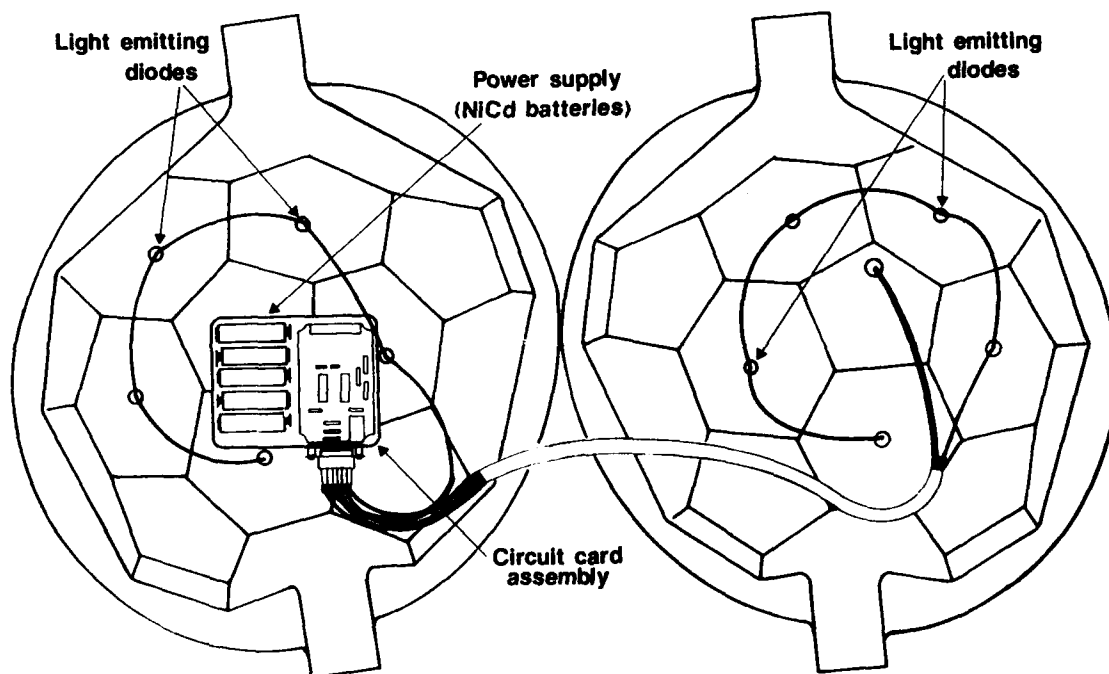Figure 3. Exterior view of solar-powered light emitting diode wire marker design.

Figure 4. Interior view of solar-powered light emitting diode wire marker design.
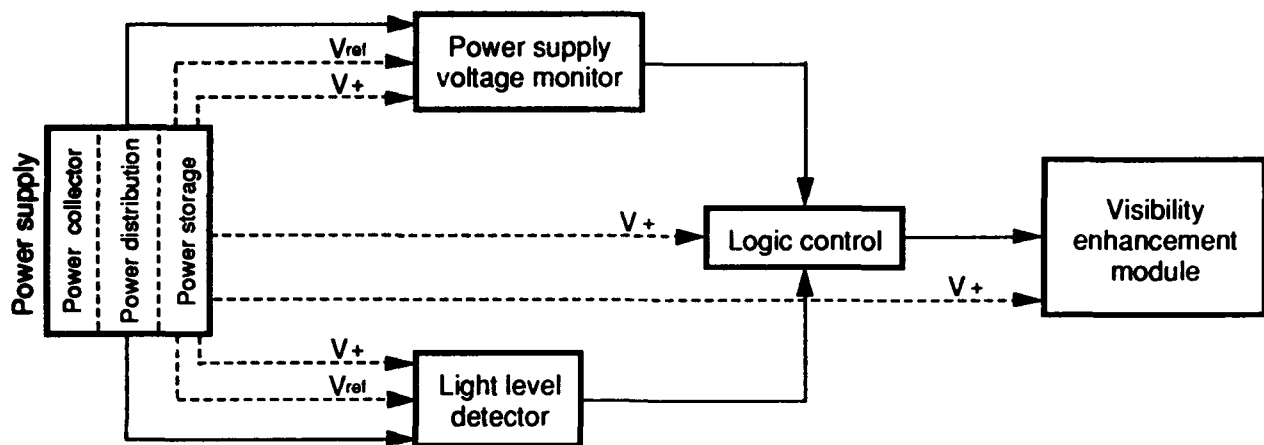
Figure 5. Wire marker design functional block diagram.

enhancement module. Alternatively, when the ambient light level drops below the threshold value, the light level detector sends appropriate logic levels to the control circuit to turn on the LED flasher circuit. Detectability of the flashing LEDs is enhanced by the retroreflective tape markers centered under each LED (see Figure 3).

The LED flasher circuit requires an operating potential of 4.0 VDC to maintain normal operation. This voltage is provided by rechargeable nickel cadmium (NiCd) batteries which are charged by the solar cells. A characteristic of NiCd batteries is consistent voltage output over the effective life of the battery. However, when power is depleted below a certain level, voltage output rapidly decreases to zero. To prevent depletion of the batteries below the circuit operating potential, the battery output voltage is continually monitored. When the battery voltage drops below 4.0 VDC, the voltage to the flashing LEDs is removed to prevent further power depletion. Excessive depletion of the NiCd batteries, which could occur during periods of continuous overcast conditions, would affect future recharging potential of the batteries.

Circuit description and operation

The solar powered LED wire marker has five distinct circuits: power supply, light level detector, power supply voltage monitor, logic control, and LED flasher. A schematic of the circuit is presented in Figure 6. A list of circuit components is provided in Appendix B.

The power supply circuit (see Figure 6) performs three functions: power collection, power storage, and power distribution. Power collection is achieved by two solar cells (3 VDC, 100 mA each) connected in series to provide 6 VDC at 100 mA. These cells are connected in parallel with four 1.2 VDC rechargeable NiCd batteries which form the power storage system.
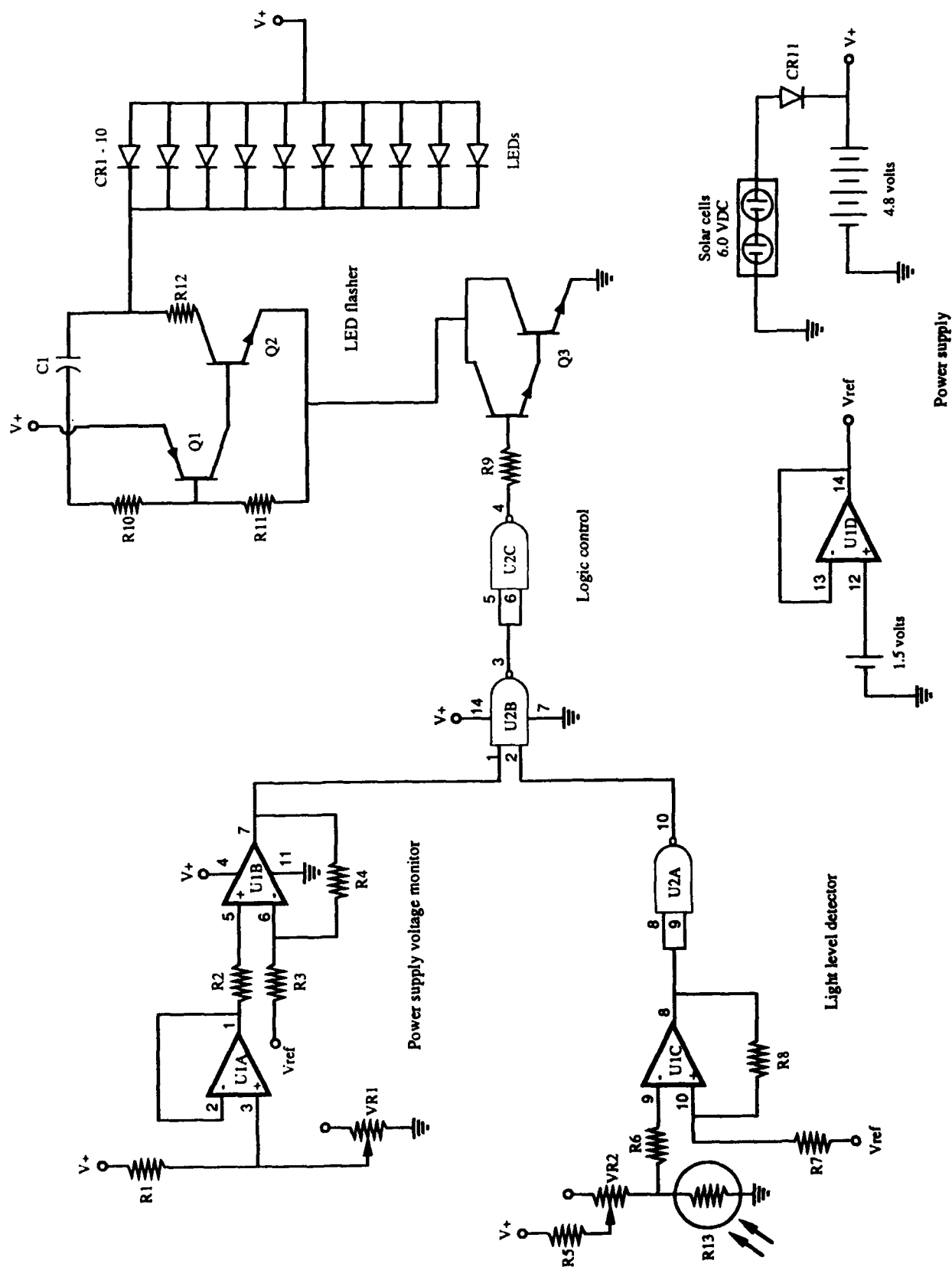
Figure 6. Schematic of solar-powered light emitting diode wire marker design.

Diode CR11 prevents battery discharge back through the solar cells during nighttime operation. The power supply provides two functional voltages. The first, V+, provides the positive operating voltage for all circuit components and signal voltages for the power supply voltage monitor and light level detector circuits. The second, V_{ref}, is a reference voltage used as a signal input to comparators in the power supply voltage monitor and light level detector circuits. V_{ref} is supplied by a single separate 1.5 VDC alkaline battery isolated by U1D ($\frac{1}{4}$-LM324N), configured as a voltage follower.

The light level detector (LLD) circuit (see Figure 6) consists of a voltage divider network containing a cadmium sulfide (CdS) photoconductive cell (photoresistor), an operational amplifier (op amp) configured as a comparator, and a NAND gate used as a logic invertor. The voltage divider network, consisting of resistor R5, potentiometer VR2, and the photoresistor R13, is used to establish a voltage level at pin 9 of op amp U1C ($\frac{1}{4}$-LM324N) which determines the point at which the transition from daytime to nighttime mode is made. For daytime operation, light falling on the photoresistor results in a low resistance value. This causes the voltage to pin 9 of U1C to go low. This low voltage at the inverting input to U1C is less than the voltage at pin 10 of U1C, the noninverting input. This latter voltage is provided from V_{ref} generated in the power supply. For these values, the output at pin 8 of U1C goes to its positive limit, V+. This high value is inverted by NAND gate U2A ($\frac{1}{4}$-CD4011BE) and becomes a low logic level which is provided to the logic control circuit. For nighttime operation, the photoresistor takes on a high resistance value. This causes the voltage to pin 9 of U1C to go high. This high voltage at the inverting input to U1C is greater than the voltage at pin 10 of U1C. For these values, the output at pin 8 of U1C goes to its negative limit. This low value is inverted by NAND gate U2A and becomes a high logic level which is provided to the logic control circuit. Potentiometer VR2 is used to adjust the daytime/nighttime transition point.

The power supply voltage monitor (PSVM) circuit (see Figure 6) consists of a voltage divider network and two op amps configured as comparators. The voltage divider consists of resistor R1 and potentiometer VR1 connected to V+ (4.8 VDC). The setting of VR1 determines the minimum battery voltage value (4.0 VDC) below which the flashing LEDs are disabled. This voltage is isolated by U1A ($\frac{1}{4}$-LM324N), configured as a voltage follower, and applied to pin 5 of U1B ($\frac{1}{4}$-LM324N). The voltage at pin 5 is compared to V_{ref} applied at pin 6 of U1B. When the battery voltage exceeds 4.0 VDC, the output at pin 7 of U1B goes high (greater than 3 VDC) and this level is provided to the logic control circuit. When the battery voltage drops below 4.0 VDC, the output of U1B goes low (less than 0.5 VDC).

9

The logic control circuit (see Figure 6) consists of two NAND gates. Logic level outputs from the PSVM and LLD circuits are applied to pins 1 and 2 of NAND gate U2B (¼-CD4011BE), respectively. The output of U2B (pin 3) is applied to pins 5 and 6 of U2C (¼-CD4011BE) which is configured as an invertor. NAND gates U2B and U2C operate together to provide an AND function of the two inputs to the logic control circuit. As long as the power supply NiCd battery voltage level is greater than 4.0 VDC, the output of the logic control circuit (pin 4 of U2C) is determined by the LLD circuit output (low for daytime and high for nighttime). If the NiCd battery voltage drops below 4.0 VDC, the resulting low input at pin 1 of U2B causes the output at pin 4 of U2C to go low. Due to the AND gate operation of the logic control circuit, its output at pin 4 of U2C is high only for the conditions of nighttime illumination and a battery voltage of greater than 4.0 VDC.

The LED flasher circuit (see Figure 6) consists of 10 LEDs, an emitter follower, a resistance-capacitance (RC) timing circuit, and several biasing and current limiting resistors. The LEDs (CR1-10) are connected together in a parallel array. The LED array is in series with V+, the timing circuit, and the emitter follower (Q3), which operates as the on/off switch for the entire LED flasher circuit. The output of the logic control circuit, applied through R9, controls the bias on Q3. For nighttime conditions and when sufficient battery voltage is available, the resulting high level at the base of Q3 forward biases Q3 and causes it to conduct. This applies a ground potential to the emitter of Q2 and the base of Q1 through resister R11. This activates the flasher timing circuit. Transistor Q1 then is biased on and off as determined by the RC time constant of resistor R10 and capacitor C1. The on and off biasing of Q1 controls the conduction of transistor Q2 which, during a portion of the period of the RC timing cycle, applies the ground potential to the LEDs through resistor R12. The LEDs are on during this period.

Bench test

Prior to full scale testing, the operational lifetime of the wire marker power supply circuit was evaluated under sustained no-light conditions. This is of interest because extended periods of inclement weather may leave the circuit switched in the nighttime (flashing) mode and not allow the solar cells to adequately recharge the NiCd cells.

The bench test was performed on a breadboard circuit with the solar cells mounted to the side. Testing was performed in a closed, unlit room. A Grant Squirrel 1200 series meter/logger was used to monitor voltages at four points in the circuit. Four channels were used to monitor the NiCd battery voltage (V+), V_{ref}

voltage (pin 14 of U1D), the power supply voltage monitor voltage (pin 7 of U1B), and the light level detector voltage (pin 10 of U2A). See Figure 6 for pin locations.

Voltage data were collected continuously over a 4-day (99 hours) period with sample readings collected and recorded at 1-minute intervals. The initial values of each parameter were V+ power supply voltage 5.29 VDC, V_{ref} voltage 1.15 VDC, PSVM voltage 3.96 VDC, and LLD voltage 4.93 VDC. Plots of these voltage data are presented in Figure 7.

Since all of the test voltages with the exception of V_{ref} were derived from V+, it was expected that changes in the power supply voltage monitor and light level detector would track with changes in V+. The curves in Figure 7 support this expectation. V+ showed a very gradual and linear decline over the first 75 hours. The rate of decline from 5.29 to 4.77 VDC during this period was approximately 7 millivolts per hour. Over the next 35 minutes, V+ dropped to 4.05 VDC at a rate of 1.4 volts per hour. Additional rapid decline occurred at 78 hours (declining to 2.98 VDC) and 85 hours (declining to 2.6 VDC). The photoresistor and PSVM output voltages showed similar trends in decline. V_{ref}, supplied by a separate battery, was unaffected by the declining V+. The test was concluded at 99 hours with final readings of 2.4 VDC at V+ and 1.15 VDC at V_{ref}.

Field test

Detection performance

During the conspicuity study cited previously, the LED design was added as an additional test design. In this test design, red LEDs were used and tested under all day/night and unaided/aided test conditions. For enhanced I^2 detectability, infrared LEDs can be used. Table 2 repeats the mean detection distances of the previously described basic and alternative designs (from Table 1). An additional column presents the detection range data of the LED design for comparison.

Each mean detection distance for the LED design was 4200 feet (the ceiling value for the test range), equaling or exceeding the values for the other test designs for *every* test condition. In a followup evaluation of the LED design for maximum detection ranges during operational flight, USAARL aviators reported being able to observe the marker with the naked eye at a distance of approximately 1000 feet at an altitude of 200 feet above ground level (AGL), approaching at 70 knots (kts).
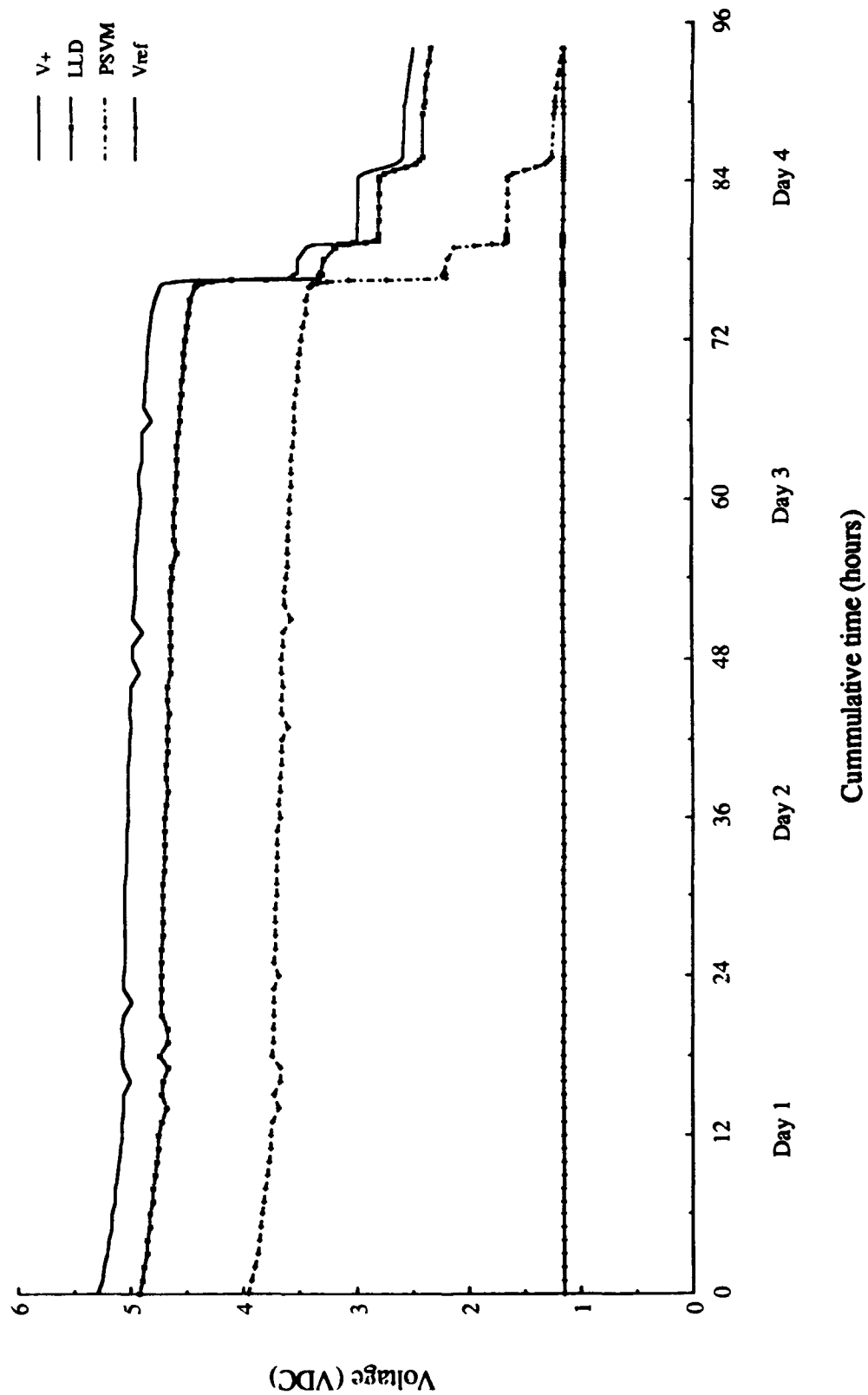
Figure 7. Output voltage plots for bench test.

Table 2.

Comparison of detection distances (in feet)
for previously tested and alternative LED designs

	Basic design	Modified basic design	Reflective polyhedron design	LED design
Day, unaided	4200*	4200*	4200*	4200*
Night, unaided Position lights	125	488	750	4200*
Anticollision lights	213	688	1225	4200*
Searchlight	1200	4200*	4200*	4200*
Blackout	63	125	138	4200*
Night, I² 2nd Position lights	450	1250	1975	4200*
Infrared searchlight	525	1375	1975	4200*
Blackout	750	825	850	4200*
Night, I² 3rd Position lights	475	1425	2050	4200*
Infrared searchlight	575	1600	2250	4200*
Blackout	750	825	950	4200*

* Note: Maximum available range was 4200 feet.

With 3rd generation image intensifiers (ANVIS), with and without anticollision lights on, the marker was observed at a distance of approximately 4300 feet at an altitude of 250 feet AGL, approaching at 70 kts. In this evaluation, the wire marker was positioned at a height of 25 feet AGL and oriented as it would be on a wire or cable. Local weather conditions were temperature of 77° F, dew point of 71° F, and relative humidity of 83 percent with scattered cloud cover at 4000 feet.
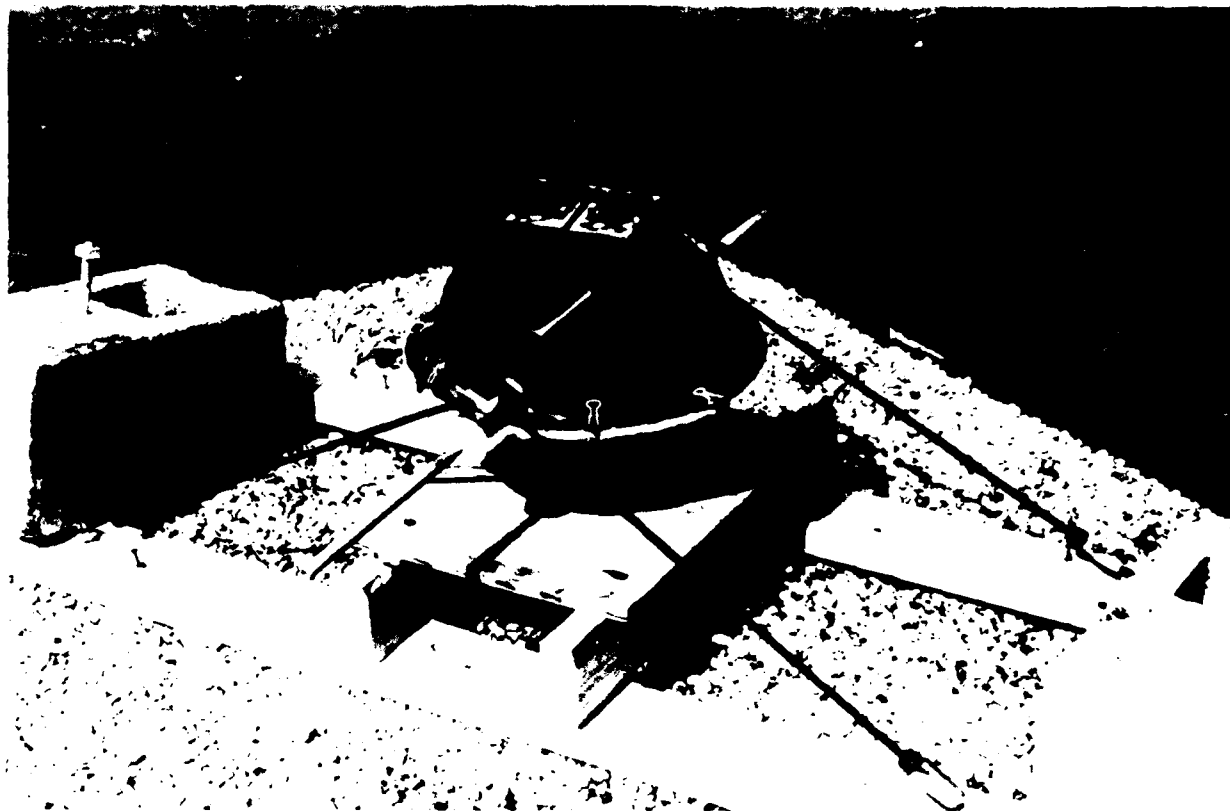
Figure 8. Operational performance test set-up of LED marker design.

Operational performance

To test the functionality of the integrated circuit for mode selection and continuous operation, a fully integrated wire marker circuit was tested in the polyhedronal shell under operational conditions. Figure 8 shows the marker setup for the operational performance testing.

Operational testing was staged at the U.S. Army Aeromedical Research Laboratory (latitude 31°10'N, longitude 85°26'W, altitude 25' AGL). The test area was a location on the roof of the building, unobscured from the sun. During the simulated operational testing, the integrated marker was maintained continually in the test area. The test was started on 10 July 1992 and ended on 14 July 1992. During this period, meteorological sunrise occurred at 0548 and sunset occurred at 1949.

A Grant Squirrel 1200 series meter/logger was used to monitor and record voltages at four points in the circuit. Four channels were monitored for solar cell voltage, NiCd battery voltage (V+), PSVM voltage (pin 7 of U1B), and LLD voltage (pin 10 of U2A).

14

Voltage data were collected continuously over a period of 96 hours beginning at 1424 on 10 July. Sample readings were taken every minute, and at each ½-hour interval, the readings were averaged and recorded by the meter/logger. The initial values of each parameter were solar cell voltage 5.84 VDC, NiCd battery (V+) voltage 5.32 VDC, PSVM voltage 4.02 VDC, and LLD op amp voltage 0.00 VDC. Plots of the voltage data recorded over the test period are presented in Figure 9.

Figure 9 shows that the weather over the test period was generally sunny to partly cloudy and 1 day was overcast with rain. Although not ideal, this weather is typical of operational conditions. During the daytime, the solar cells did not reach full potential (6.0 VDC), but they maintained average values of 5.49 VDC to 5.75 VDC which was adequate to charge the four 1.3 volt batteries. As ambient lighting was reduced or increased, the solar cell voltages gradually changed towards a low value of zero volts or a high value of six volts, respectively. Data showed that the most significant rates of voltage change occurred in the two 30-minute periods prior to switch to nighttime mode, and in the one 30-minute period subsequent to switch to daytime mode. During the day, small voltage fluctuations occurred due to cloud cover.

While the solar cell voltages were above the total NiCd battery voltage (5.2 VDC), the batteries (V+) were charged. This was indicated by the rise in V+ during the daytime and the gradual decline as the sun set into the nighttime. The average daytime voltages of V+ ranged from 5.35 VDC to 5.40 VDC, and the average nighttime voltages ranged from 5.12 VDC to 5.16 VDC. Throughout this testing period, the batteries maintained a voltage no lower than 5.03 VDC, which occurred at the end of a nighttime cycle.

Because the power supply voltage monitor circuit was designed to monitor the battery voltage, the increases and decreases in V+ voltage were reflected in the PSVM. The PSVM average daytime voltage values ranged from 4.08 VDC to 4.12 VDC, and the average nighttime voltage values ranged from 3.81 VDC to 3.83 VDC. The PSVM and V+ voltages consistently differed by approximately 1.31 volts and, since the V+ voltage remained above 4.00 VDC throughout the test period, the PSVM voltages never dropped below 3.00 volts (as designed).

In the daytime, the photoresistor in the light level detector circuit had a low resistance value so that the LLD voltage had a value of zero. At nighttime, the average voltages ranged from 5.09 VDC to 5.12 VDC. The voltages across the LLD circuit at night were equivalent to the V+ voltages until transition occurred.
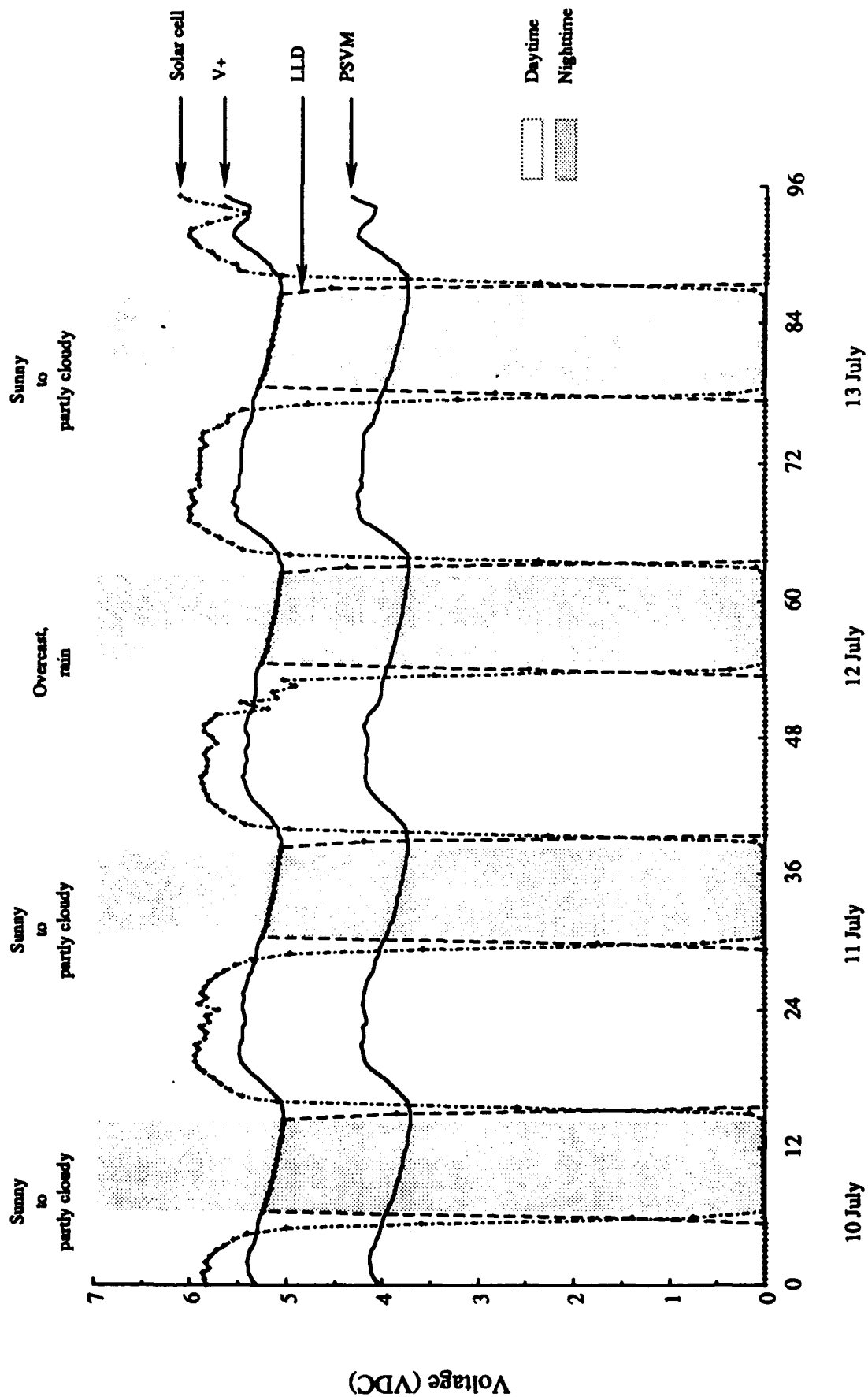
Figure 9. Output voltage plots for operational performance test.

16

The transition from daytime to nighttime mode was instantaneous once the ambient lighting fell below a level determined by the user. Under normal operation, the light level detector circuit controlled the switch. In the daytime, the photoresistor in the LLD circuit had a low resistance value of zero. At nighttime, the average voltages ranged from 5.09 to 5.12 VDC. The nighttime voltages were equivalent to the V+ voltages until transition occurred. The curve of LLD in Figure 9 has a sloped appearance due to the averaging of voltages over a 30-minute period. The transition between modes occurred in the last 30 minutes of each day/night period. From the data, a switch was determined to have occurred when voltage values of the LLD circuit rose to the V+ voltage (transition to night mode) or dropped below the V+ voltage (transition to day mode).

During the test period, the temperature and humidity were high. The photo in Figure 8 shows some condensation occurring inside the solar cell packages. Data showed that the performance of the solar cells was not affected by the moisture. On the afternoon of the third testing day, an episode of torrential rain occurred where the solar cell voltages changed irregularly (see Figure 9) due to heavy intermittent overcast. Data on the following day appeared nominal and water was not found inside the marker shell at the conclusion of testing.

Summary

The self-powered light emitting diode wire marker is an alternative marker intended for use in indicating the presence of cables and/or wires located at heights above the ground which could be potential aviation hazards. Current wire markers employ an international-orange color with reflective or retroreflective marking patterns to augment visibility and detection range. This alternative marker design enhances visibility and detection range over the current design through the use of active emission light emitting diodes which are visible to the naked eye and image intensification systems.

Enhanced detectability is the predominant advantage of this alternative wire marker design. Another significant feature of this LED marker is the powering circuit which is designed to recharge itself and automatically select the operating mode based on ambient lighting conditions. A photodetector monitors ambient light levels and regulates switching between daytime mode (when the solar cells recharge the batteries and the LEDs are switched off) and nighttime/adverse weather mode (when the LEDs are switched on to flash).

In a controlled laboratory bench test of the powering circuit, it was determined that four rechargeable NiCd batteries were capable of supporting the circuit in continuous nighttime

(LED flashing) mode for a period of 75 hours before unrecoverable failure of the batteries occurred. Operational performance testing showed that two 3-volt solar cells were sufficient for maintaining battery charge under normal operating conditions, and that the mode selection circuit operated successfully in switching the circuit for most efficient operation over five periods of daytime and four periods of nighttime operation. This test also showed that the shell integrated with the solar cells, photodetector, and LEDs provided protection from heat and water.

Results of the bench test and operational performance test indicate that this alternative self-powering LED wire marker system is a feasible alternative for current markers to provide low-maintenance, enhanced detectability of wire and/or cable hazards to aviation.

Reference

Levine, R. R., Rash, C. E., and Martin, J. S. 1991. _Conspicuity comparison of current and proposed U.S. Army wire marker designs_. USAARL Report No. 91-9.

Appendix A.

List of manufacturers

3M Traffic Control Materials Division
Building 223-3N-01, 3M Center
St. Paul, MN 55144-1000

Grant Instruments (Cambridge) Ltd.
Barrington, Cambridge CB2 5QZ England
for Science/Electronics
2277 Maue Rd.
Miamisburg, Ohio 45342

Appendix B.

List of components

C1   Capacitor, electrolytic, 4.7 μF, 35 V
CR1-10   Light emitting diode, CX556R
CR11 Diode, germanium, 1N34A, 75 V PIV
Q1   Transistor, 2N2907
Q2   Transistor, 2N2222
Q3   Transistor, ECG265, Darlington
R1   Resistor, 100K Ω, ¼ watt, 1%
R2, R6   Resistor, 39K Ω, ¼ watt, 1%
R3, R7   Resistor, 47K Ω, ¼ watt, 1%
R4, R8-11   Resistor,   1K Ω, ¼ watt, 1%
R5   Resistor, 33K Ω, ¼ watt, 1%
R12   Resistor,   10 Ω, ¼ watt, 5%
U1A   Quad op amp, LM324N
U2A   Quad NAND gate, CD4011BE
VR1-2 Potentiometer, 100K Ω, 15 turn, 3/4 watt

Battery alkaline, 1.5 VDC
Battery (4)   NiCd, rechargeable, 1.2 VDC
CdS cell photoconductive cell (photoresistor), CL703L/2,
      dual element
Photovoltaic
  Cell (2)   Solar cell, 3 VDC, 100 mA

Initial distribution

Commander, U.S. Army Natick Research,
  Development and Engineering Center
ATTN: SATNC-MIL (Documents
  Librarian)
Natick, MA 01760-5040

U.S. Army Communications-Electronics
 Command
ATTN: AMSEL-RD-ESA-D
Fort Monmouth, NJ 07703

Commander/Director
U.S. Army Combat Surveillance
  and Target Acquisition Lab
ATTN: DELCS-D
Fort Monmouth, NJ 07703-5304

Commander
10th Medical Laboratory
ATTN: Audiologist
APO New York 09180

Naval Air Development Center
Technical Information Division
Technical Support Detachment
Warminster, PA 18974

Commanding Officer, Naval Medical
  Research and Development Command
National Naval Medical Center
Bethesda, MD 20814-5044

Deputy Director, Defense Research
  and Engineering
ATTN: Military Assistant
  for Medical and Life Sciences
Washington, DC 20301-3080

Commander, U.S. Army Research
  Institute of Environmental Medicine
Natick, MA 01760

Library
Naval Submarine Medical Research Lab
Box 900, Naval Sub Base
Groton, CT 06349-5900

Director, U.S. Army Human
  Engineering Laboratory
ATTN: Technical Library
Aberdeen Proving Ground, MD 21005

Commander
Man-Machine Integration System
Code 602
Naval Air Development Center
Warminster, PA 18974

Commander
Naval Air Development Center
ATTN: Code 602-B (Mr. Brindle)
Warminster, PA 18974

Commanding Officer
Armstrong Laboratory
Wright-Patterson
Air Force Base, OH 45433-6573

Director
Army Audiology and Speech Center
Walter Reed Army Medical Center
Washington, DC 20307-5001

Commander, U.S. Army Institute
  of Dental Research
ATTN: Jean A. Setterstrom, Ph. D.
Walter Reed Army Medical Center
Washington, DC 20307-5300

Naval Air Systems Command
Technical Air Library 950D
Room 278, Jefferson Plaza II
Department of the Navy
Washington, DC 20361

Commander, U.S. Army Test
and Evaluation Command
ATTN: AMSTE-AD-H
Aberdeen Proving Ground, MD 21005

Director
U.S. Army Ballistic
Research Laboratory
ATTN: DRXBR-OD-ST Tech Reports
Aberdeen Proving Ground, MD 21005

Commander
U.S. Army Medical Research
Institute of Chemical Defense
ATTN: SGRD-UV-AO
Aberdeen Proving Ground,
MD 21010-5425

Commander, U.S. Army Medical
Research and Development Command
ATTN: SGRD-RMS (Ms. Madigan)
Fort Detrick, Frederick, MD 21702-5012

Director
Walter Reed Army Institute of Research
Washington, DC 20307-5100

HQ DA (DASG-PSP-O)
5109 Leesburg Pike
Falls Church, VA 22041-3258

Harry Diamond Laboratories
ATTN: Technical Information Branch
2800 Powder Mill Road
Adelphi, MD 20783-1197

U.S. Army Materiel Systems
Analysis Agency
ATTN: AMXSY-PA (Reports Processing)
Aberdeen Proving Ground
MD 21005-5071

U.S. Army Ordnance Center
and School Library
Simpson Hall, Building 3071
Aberdeen Proving Ground, MD 21005

U.S. Army Environmental
Hygiene Agency
Building E2100
Aberdeen Proving Ground, MD 21010

Technical Library Chemical Research
and Development Center
Aberdeen Proving Ground, MD
21010--5423

Commander
U.S. Army Medical Research
Institute of Infectious Disease
SGRD-UIZ-C
Fort Detrick, Frederick, MD 21702

Director, Biological
Sciences Division
Office of Naval Research
600 North Quincy Street
Arlington, VA 22217

Commander
U.S. Army Materiel Command
ATTN: AMCDE-XS
5001 Eisenhower Avenue
Alexandria, VA 22333

Commandant
U.S. Army Aviation
Logistics School ATTN: ATSQ-TDN
Fort Eustis, VA 23604

Headquarters (ATMD)
U.S. Army Training
and Doctrine Command
ATTN: ATBO-M
Fort Monroe, VA 23651

Structures Laboratory Library
USARTL-AVSCOM
NASA Langley Research Center
Mail Stop 266
Hampton, VA 23665

Naval Aerospace Medical
  Institute Library
Building 1953, Code 03L
Pensacola, FL 32508-5600

Command Surgeon
HQ USCENTCOM (CCSG)
U.S. Central Command
MacDill Air Force Base FL 33608

Air University Library
(AUL/LSE)
Maxwell Air Fore Base, AL 36112

U.S. Air Force Institute
  of Technology (AFIT/LDEE)
Building 640, Area B
Wright-Patterson
Air Force Base, OH 45433

Henry L. Taylor
Director, Institute of Aviation
University of Illinois-Willard Airport
Savoy, IL 61874

Chief, Nation Guard Bureau
ATTN: NGB-ARS (COL Urbauer)
Room 410, Park Center 4
4501 Ford Avenue
Alexandria, VA 22302-1451

Commander
U.S. Army Aviation Systems Command
ATTN: SGRD-UAX-AL (LTC Gillette)
4300 Goodfellow Blvd., Building 105
St. Louis, MO 63120

U.S. Army Aviation Systems Command
  Library and Information Center Branch
ATTN: AMSAV-DIL
4300 Goodfellow Boulevard
St. Louis, MO 63120

Federal Aviation Administration
Civil Aeromedical Institute
Library AAM-400A
P.O. Box 25082
Oklahoma City, OK 73125

Commander
U.S. Army Academy
  of Health Sciences
ATTN: Library
Fort Sam Houston, TX 78234

Commander
U.S. Army Institute of Surgical Research
ATTN: SGRD-USM (Jan Duke)
Fort Sam Houston, TX 78234-6200

AAMRL/HEX
Wright-Patterson
Air Force Base, OH 45433

John A. Dellinger,
Southwest Research Institute
P. 0. Box 28510
San Antonio, TX 78284

Product Manager
Aviation Life Support Equipment
ATTN: AMCPM-ALSE
4300 Goodfellow Boulevard
St. Louis, MO 63120-1798

Commander
U.S. Army Aviation
  Systems Command
ATTN: AMSAV-ED
4300 Goodfellow Boulevard
St. Louis, MO 63120

Commanding Officer
Naval Biodynamics Laboratory
P.O. Box 24907
New Orleans, LA 70189-0407

Assistant Commandant
U.S. Army Field Artillery School
ATTN: Morris Swott Technical Library
Fort Sill, OK 73503-0312

Commander
U.S. Army Health Services Command
ATTN: HSOP-SO
Fort Sam Houston, TX 78234-6000

HQ USAF/SGPT
Bolling Air Force Base, DC 20332-6188

U.S. Army Dugway Proving Ground
Technical Library, Building 5330
Dugway, UT 84022

U.S. Army Yuma Proving Ground
Technical Library
Yuma, AZ 85364

AFFTC Technical Library
6510 TW/TSTL
Edwards Air Force Base,
CA 93523-5000

Commander
Code 3431
Naval Weapons Center
China Lake, CA 93555

Aeromechanics Laboratory
U.S. Army Research and Technical Labs
Ames Research Center, M/S 215-1
Moffett Field, CA 94035

Sixth U.S. Army
ATTN: SMA
Presidio of San Francisco, CA 94129

Commander
U.S. Army Aeromedical Center
Fort Rucker, AL 36362

U.S. Air Force School
  of Aerospace Medicine
Strughold Aeromedical Library Technical
Reports Section (TSKD)
Brooks Air Force Base, TX 78235-5301

Dr. Diane Damos
Department of Human Factors
ISSM, USC
Los Angeles, CA 90089-0021

U.S. Army White Sands
  Missile Range
ATTN: STEWS-IM-ST
White Sands Missile Range, NM 88002

U.S. Army Aviation Engineering
  Flight Activity
ATTN: SAVTE-M (Tech Lib) Stop 217
Edwards Air Force Base, CA 93523-5000

Ms. Sandra G. Hart
Ames Research Center
MS 262-3
Moffett Field, CA 94035

Commander, Letterman Army Institute
  of Research
ATTN: Medical Research Library
Presidio of San Francisco, CA 94129

Commander
U.S. Army Medical Materiel
  Development Activity
Fort Detrick, Frederick, MD 21702-5009

Commander
U.S. Army Aviation Center
Directorate of Combat Developments
Building 507
Fort Rucker, AL 36362

U. S. Army Research Institute
Aviation R&D Activity
ATTN: PERI-IR
Fort Rucker, AL 36362

Commander
U.S. Army Safety Center
Fort Rucker, AL 36362

U.S. Army Aircraft Development
  Test Activity
ATTN: STEBG-MP-P
Cairns Army Air Field
Fort Rucker, AL 36362

Commander U.S. Army Medical Research
  and Development Command
ATTN: SGRD-PLC (COL Schnakenberg)
Fort Detrick, Frederick, MD 21702

MAJ John Wilson
TRADOC Aviation LO
Embassy of the United States
APO New York 09777

Netherlands Army Liaison Office
Building 602
Fort Rucker, AL 36362

British Army Liaison Office
Building 602
Fort Rucker, AL 36362

Italian Army Liaison Office
Building 602
Fort Rucker, AL 36362

Directorate of Training Development
Building 502
Fort Rucker, AL 36362

Chief
USAHEL/USAAVNC Field Office
P. O. Box 716
Fort Rucker, AL 36362-5349

Commander U.S. Army Aviation Center
  and Fort Rucker
ATTN: ATZQ-CG
Fort Rucker, AL 36362

Chief
Test & Evaluation Coordinating Board
Cairns Army Air Field
Fort Rucker, AL 36362

MAJ Terry Newman
Canadian Army Liaison Office
Building 602
Fort Rucker, AL 36362

German Army Liaison Office
Building 602
Fort Rucker, AL 36362

LTC Patrice Cottebrune
French Army Liaison Office
USAAVNC (Building 602)
Fort Rucker, AL 36362-5021

Australian Army Liaison Office
Building 602
Fort Rucker, AL 36362

Dr. Garrison Rapmund
6 Burning Tree Court
Bethesda, MD 20817

Commandant, Royal Air Force
Institute of Aviation Medicine
Farnborough Hampshire GU14 6SZ UK

Commander
U.S. Army Biomedical Research
  and Development Laboratory
ATTN: SGRD-UBZ-I
Fort Detrick, Frederick, MD 21702

Defense Technical Information
Cameron Station, Building 5
Alexandria, VA 22304-6145

Commander, U.S. Army Foreign Science
and Technology Center
AIFRTA (Davis)
220 7th Street, NE
Charlottesville, VA 22901-5396

Director,
Applied Technology Laboratory
USARTL-AVSCOM
ATTN: Library, Building 401
Fort Eustis, VA 23604

U.S. Air Force Armament
Development and Test Center
Eglin Air Force Base, FL 32542

Commander, U.S. Army Missile
Command
Redstone Scientific Information Center
ATTN: AMSMI-RD-CS-R
/ILL Documents
Redstone Arsenal, AL 35898

Dr. H. Dix Christensen
Bio-Medical Science Building, Room 753
Post Office Box 26901
Oklahoma City, OK 73190

Director
Army Personnel Research Establishment
Farnborough, Hants GU14 6SZ UK

U.S. Army Research and Technology
Laboratories (AVSCOM)
Propulsion Laboratory MS 302-2
NASA Lewis Research Center
Cleveland, OH 44135

Dr. Christine Schlichting
Behavioral Sciences Department
Box 900, NAVUBASE NLON
Groton, CT 06349-5900

Dr. Eugene S. Channing
7985 Schooner Court
Frederick, MD 21701-3273

LTC Gaylord Lindsey (5)
USAMRDC Liaison at Academy
of Health Sciences
ATTN: HSHA-ZAC-F
Fort Sam Houston, TX 78234

Aviation Medicine Clinic
TMC #22, SAAF
Fort Bragg, NC 28305

Dr. A. Kornfield, President
Biosearch Company
3016 Revere Road
Drexel Hill, PA 29026

NVEOD
AMSEL-RD-ASID
(Attn: Trang Bui)
Fort Belvior, VA 22060

CA Av Med
HQ DAAC
Middle Wallop
Stockbridge Hants S020 8DY UK

Commander and Director
USAE Waterways Experiment Station
ATTN: CEWES-IM-MI-R
Alfrieda S. Clark, CD Dept.
3909 Halls Ferry Road
Vicksburg, MS 39180-6199

Mr. Richard Thornley
ILS Manager, APACHE
Box 84
Westland Helicopters Limited
Yeovil, Somerset BA202YB UK

Col. Otto Schramm Filho
c/o Brazilian Army Commission
Office-CEBW
4632 Wisconsin Avenue NW
Washington, DC 20016